ChemPubSoc Europe

DOI: 10.1002/ejic.201700535

EurJIC European Journal of Inorganic Chemistry

Full Paper

Supramolecular Chemistry | *Very Important Paper* |

CLUSTER ISSUE

VIP

Crystalline Inclusion Compounds of a Palladacyclic Tetraol Host Featuring *o*-Carborane Units

Min Ying Tsang,[a] Clara Viñas,[a] Francesc Teixidor,[a] Duane Choquesillo-Lazarte,[b] and José Giner Planas*[a]

Abstract: A new neutral host Pd_2L_2 metallacycle, featuring a bulky bis[3-pyridyl(hydroxy)methyl]-1,2-dicarba-*closo*-dodecaborane, is synthesized, and seven crystalline inclusion compounds are obtained from DMF, DMSO, EtOAc, and THF, with the last four acting as guest solvents. Single-crystal X-ray diffraction structural analysis shows the formation of 1:*n* (*n* = 6–8) host/guest crystals, indicating a high stoichiometric ratio of included solvent. Single-crystal X-ray diffraction analyses of all structures reveal a supramolecular ordering of the palladacycles in the solid state, through extensive hydrogen bonding or intermolecular contacts, mainly between the host and the guest molecules.

Introduction

The design and self-assembly of hydrogen-bond-containing synthons is a very relevant research activity in supramolecular chemistry and crystal engineering.[1] Selective formation of crystalline inclusion compounds is one of the main challenges in this area of research.[2] A successful strategy for designing host compounds that entraps molecular guests in their crystal lattice consists of synthesizing awkwardly shaped molecules that can only pack inefficiently in the solid state.[2,3] Furthermore, decoration of the host with functional groups capable of hydrogen bonding often improves the inclusion properties.

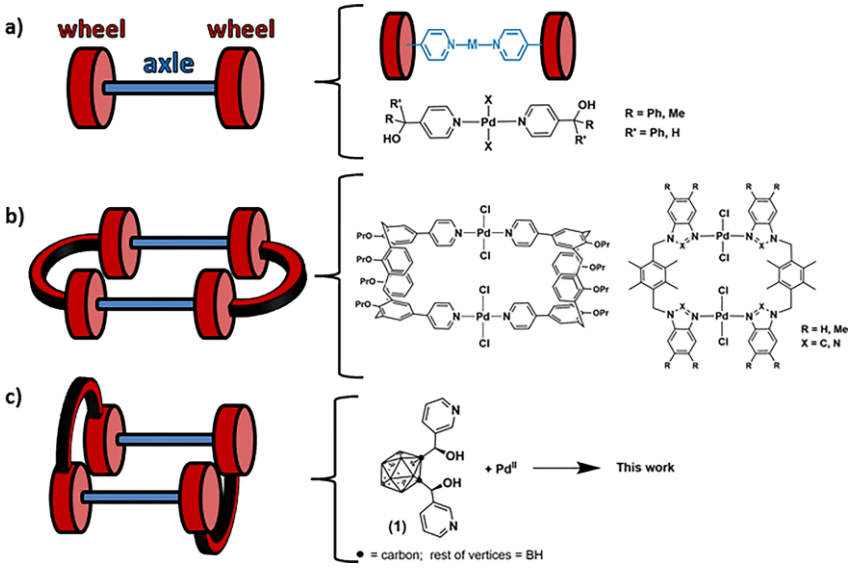

Figure 1. Schematic representation and selected examples of: (a) wheel-and-axle metal–organic diols (WAMODs); (b) double-wheel-and-axle or rectangular metallacycles; and (c) this work. See full text for references.

[a] *Institut de Ciència de Materials de Barcelona (ICMAB-CSIC), Campus UAB, 08193 Bellaterra, Spain*
E-mail: jginerplanas@icmab.es
https://departments.icmab.es/lmi/
[b] *Laboratorio de Estudios Cristalográficos, IACT, CSIC – Universidad de Granada, Avenida de las Palmeras 4, 18100 Armilla, Granada, Spain*
Supporting information and ORCID(s) from the author(s) for this article are available on the WWW under https://doi.org/10.1002/ejic.201700535.

Wheel-and-axle molecular geometries (Figure 1), first reported by Toda,[4] correspond to this line of reasoning.[3,5] Such molecular geometries are produced by connecting two bulky propeller-shaped groups by a long linker (for short linkers, they are known as the dumbbell[2a] type). These types of compounds have been developed into a large family of purely organic-based hosts for lattice-inclusion compounds with variations in

the end groups (wheels) and/or central linear building block (axle).[2a,3,6] When the axle groups are decorated with hydrogen-bonding functional groups such as alcohols, they are termed "wheel-and-axle" diols.[4a] A considerable innovation in this field was the introduction of a metal in these wheel-and-axle compounds, either at the wheels or at the axle (top of Figure 1).[7] For example, the metal can be part of the axle through classical coordination bonds, as in the series of wheel-and-axle metal–organic diols (WAMODs) shown in Figure 1. In these compounds, monodentate pyridine alcohols form metal complexes, mainly from palladium, to provide a large family of PdL_2X_2 inclusion compounds. In an increasing level of complexity, the use of dipyridine ligands as end groups (wheels) has provided a variety of Pd_2L_2-type metallacycles with varying axle-to-axle distances.[6b,8] Although some of these metallacycles have been considered wheel-and-axle types, a simple representation of those (middle of Figure 1) suggests that they can be better regarded as double-wheel-and-axle or simply rectangular metallacycles. Such metallacycles are of interest as molecular containers or receptors when they have central cavities and still show inclusion behavior for aromatic guests or other smaller molecules.[6b,8c,8d,8f]

The host compound presented in this paper belongs to the Pd_2L_2-type metallacycles, but it has a building unit distinct from those of the previously mentioned metallacycles. In particular, it contains a disubstituted *o*-carboranyl alcohol, bearing two 3-pyridyl moieties (**1** in Figure 1).[9] The high thermal and chemical stability, hydrophobicity, acceptor character, ease of functionalization, and three-dimensional nature of the icosahedral carborane clusters (*closo*-$C_2B_{10}H_{12}$) make these new molecules valuable ligands in chemistry and materials science.[10] These icosahedral molecules are versatile building blocks in supramolecular chemistry, capable of establishing a variety of conventional and nonconventional hydrogen bonding.[11] The incorporation of carboranes as functional moieties in supramolecular chemistry has been a desirable goal, with the expectation that the resulting assemblies will exhibit interesting properties.[10f,12] We have been particularly interested in relating the field of molecular crystal engineering with that of icosahedral carboranes.[9b,9c,11a,13] It is surprising that, taking into account the rich supramolecular chemistry and bulkiness of icosahedral carborane derivatives, crystalline lattice-inclusion compounds have been hardly reported.[11i,14] Compound **1**, which is prepared in very good yield from one-pot reactions and from readily available starting materials,[10a] is centered on an *o*-carborane core with one or two arms radiating out of one of the cluster carbons, containing a carbon that bears an alcohol and a 3-pyridyl moiety. The arrangement of the pyridyl moieties

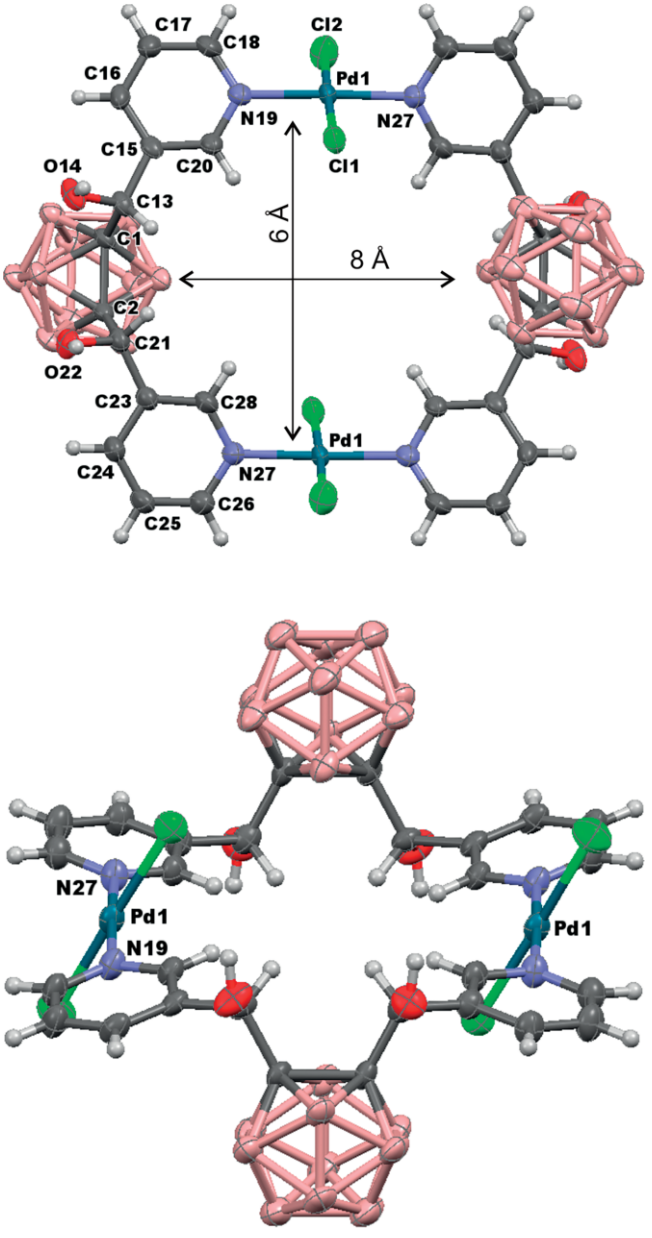

Figure 2. Labelled ORTEP diagrams for two different views of **2**·DMF-I. The thermal ellipsoids are shown at the 80 % probability level and the H atoms are shown as fixed-size spheres of 0.18 Å. The DMF molecules and H atoms attached to boron (pink) are omitted for clarity.

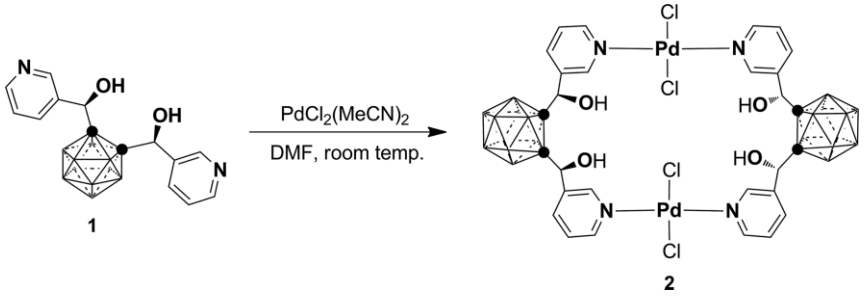

Scheme 1. Synthesis of **2**.

in this compound, from the single-crystal X-ray diffraction structural analysis,[9c] suggests that it could act as a bidentate ligand for the construction of metallacyclic structures.[12b,15] The lower symmetry (Cs) and awkward shape of our carboranyl ligand, compared with most of the reported bidentate pyridines (C_2 symmetry), could provide lower symmetry and a more awkward shape of the corresponding Pd_2L_2-type metallacycles, and therefore, inclusion properties. The combination of the latter with the central cavities originating from the rectangular palladacyclic compounds, and the presence of four alcohol groups, might enhance the inclusion properties of this host. In the present work, we report the palladium-containing metallacycle from **1** and seven different crystalline lattice-inclusion compounds (Scheme 1 and Figure 2), with exceptionally high host/guest stoichiometric ratios of 1:*n* (*n* = 6–8). We provide a detailed discussion of the X-ray diffraction crystal structures and inclusion properties for these compounds.

Results and Discussion

Reaction of equimolar amounts of $[PdCl_2(CH_3CN)_2]$ with ligand **1** gave the corresponding neutral dipalladium(II) complex **2** in high yield, as shown in Scheme 1. Note that the *syn*-diastereoisomer of **1** is used in this work (see Exp. Sect.). Compound **2** is only slightly soluble in very polar solvents (vide infra). Compound **2** has been fully characterized by standard spectroscopic techniques (see Exp. Sect.) and the data correlated well with that of related palladium complexes.[10g]

Since the palladacyclic dimer possesses four hydroxyl groups that are not involved in the complex formation, it was expected that compound **2** would show inclusion behavior. Compound **2** is insoluble in water, acetone, acetonitrile, 1,4-dioxane, diethyl ether, dichloromethane, or *n*-hexane. It is, however, slightly soluble in very polar organic solvents and does form inclusion compounds from DMF, DMSO, THF, and EtOAc. The different lattice-inclusion compounds were obtained by carrying the reaction of **1** with $[PdCl_2(CH_3CN)_2]$ in the appropriate solvent or by recrystallization of **2**·DMF crystals (see Exp. Sect.). These procedures afforded crystals for seven inclusion compounds: **2**·DMF-I, **2**·DMF-II, **2**·DMSO-I, **2**·DMSO-II, **2**·DMF/DMSO, **2**·EtOAc, and **2**·THF. The structures for all inclusion compounds have been unequivocally established by X-ray diffraction crystallography. Crystal and data collection details can be found in Table 1 and in the Exp. Sect. Solvents of crystallization, host/guest stoichiometry, space groups, calculated densities, and guest-accessible volumes are given in Table 2.

X-ray Crystal Structures and Inclusion Behavior

The inclusion compounds can be grouped into three isostructural structures: Group 1: **2**·DMF-I, **2**·DMSO-I, **2**·DMF/DMSO, and **2**·EtOAc crystallized in the space group $P\bar{1}$, with $Z = 1$ and similar cell dimensions (Table 1); Group 2: **2**·DMF-II and **2**·DMSO-II in the space group $P2_1/n$, with $Z = 2$; and Group 3: **2**·THF crystallized in the space group $P2_1/c$, with $Z = 2$. A comparison of the eight crystal structures of the inclusion compounds of **2** revealed a remarkably constant conformation of the host molecule **2** in all the structures (see Supporting Information for molecular overlap, Figure S1). The structural analyses confirmed that all complexes form discrete M_2L_2-type metallacycles, consisting of two $PdCl_2$ units bridged by two ligands (**1**), through the pyridine N atoms, each acting as a molecular clip. Figure 2 shows, as an example, a molecule of the host from the structure **2**·DMF-I. In all structures, ligand **1** adopts a *cis* arrangement of the pyridine rings, and this determines the shape of the metallacycles. The $Pd_2L_2Cl_4$ metallacycles lie on an inversion center that is located in the middle of the metallacycle. Consequently, the carboranyl alcohol moieties lie on opposite sides of the metallacycle ring, which, in addition, contains a significant rectangular central cavity (ca. 8 × 6 Å; see Figure 2). Both N atoms and Cl^- donors are *trans* in each palladium, leading to a square-planar coordination geometry of the Pd^{2+} ions, with N–Pd–N and Cl–Pd–Cl angles in the ranges 177.9–179.5° and 175.0–177.8°, respectively. The Pd–N and Pd–Cl bond lengths fall in the ranges 2.01–2.04 and 2.28–2.31 Å, respectively. Some DMSO or EtOAc molecules in **2**·DMF/DMSO, **2**·DMSO-II, or **2**·EtOAc, respectively, were partially disordered, so that the solvent-masking procedure implemented in Olex2[16] was used to remove the electronic contribution of solvent molecules from the refinement (Table 2 and Exp. Sect.). Interestingly, **2**·DMF-I and **2**·DMF-II show the same host/guest ratio and are true polymorphs.

The possibility of solving the X-ray diffraction crystal structures of the different inclusion compounds of **2** (Figure 3) allowed us to further analyze the nature of the host–guest interactions (Table 3 and Figures S2,S3). The solid-state structures for the eight inclusion compounds presented in this work constitute examples of lattice-inclusion compounds with small molecular guests.[17] One remarkable point is the host/guest stoichiometric ratios of 1:6 to 1:8, which are exceptionally high, with respect to the guest component. The latter indicates a high guest-accommodation efficiency.

Guest molecules are found in three different places, with respect to the palladacyclic ring (formula): (1) on the hydroxyl groups (*on-guest*); (2) inside the palladacycle (*in-guest*); and (3) outside the palladacycle (*out-guest*). Detailed analyses of host–guest intermolecular contacts (Table 3 and Figures S2,S3) reveals that whereas the *on-guest* solvent molecules are hydrogen bonded to the OH moieties of the palladacycle by O–H···O interactions, the *in-* and *out-guest* solvent molecules are interacting with the palladacycle through weaker C–H···O, and in some cases, C–H···H–B contacts.[11f,13c,13d]

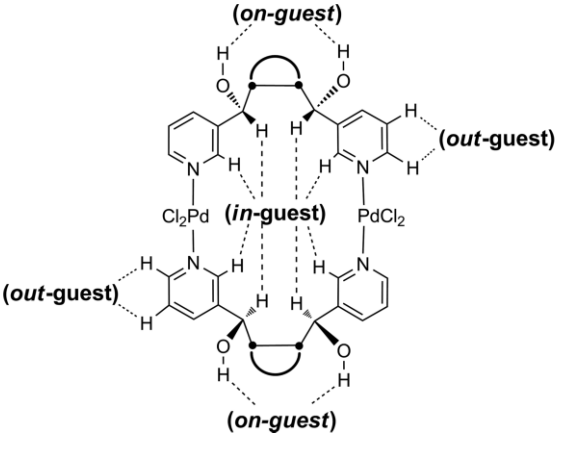

As expected, guest molecules are acting as hydrogen-bond acceptors, being the *on-guest* molecules involved in (host)-O–H···O(guest) moderate hydrogen bonds (O–H···O hydrogen bonds with O···O distances and O–H–O angles in the ranges

Table 1. Crystal data and refinement details for compounds **2**·DMF-I, **2**·DMF-II, **2**·DMSO-I, **2**·DMSO-II, **2**·DMF/DMSO, **2**·EtOAc, and **2**·THF.

	2·DMF-I	**2**·DMF-II	**2**·DMSO-I	**2**·DMSO-II
Empirical formula	$C_{28}H_{44}B_{10}Cl_4N_2O_4Pd_2$·6DMF	$C_{28}H_{44}B_{10}Cl_4N_2O_4Pd_2$·6DMF	$C_{28}H_{44}B_{10}Cl_4N_2O_4Pd_2$·8DMSO	$C_{28}H_{44}B_{10}Cl_4N_2O_4Pd_2$·7DMSO
Formula weight	1510.05	1510.05	1696.50	1618.37
Crystal system	triclinic	monoclinic	triclinic	monoclinic
Space group	$P\bar{1}$	$P2_1/n$	$P\bar{1}$	$P2_1/n$
Unit cell dimensions [Å, °]	a = 10.9693(2)	a = 17.3172(17)	a = 10.9878(10)	a = 9.6190(5)
	b = 12.0415(3)	b = 11.0888(10)	b = 11.1304(10)	b = 19.8802(10)
	c = 14.6057(3)	c = 19.719(2)	c = 16.2174(15)	c = 19.0729(9)
	α = 68.9850(10)		α = 106.183(3)	
	β = 73.2720(10)	β = 107.694(4)	β = 94.722(4)	β = 97.050(2)
	γ = 85.4180(10)		γ = 93.595(4)	
Volume [Å^3]	1724.10(6)	3607.5(6)	1890.7(3)	3619.7(3)
Z	1	2	1	2
$\varrho_{calcd.}$ [g cm^{-3}]	1.454	1.390	1.490	1.485
Absorption coeff. [mm^{-1}]	6.099	0.702	7.632	7.672
F(000)	772	1544	868	1652
Crystal	block, yellow	block, yellow	block, yellow	block, yellow
Crystal size [mm]	0.58 × 0.43 × 0.30	0.12 × 0.1 × 0.1	0.12 × 0.10 × 0.10	0.08 × 0.07 × 0.07
θ range for data collection [°]	3.37–65.50	2.29–25.02	2.85–66.59	3.22–66.50
Reflections collected	18273	15427	28900	6066
Independent reflections	5676 [R_{int} = 0.0551]	6286 [= 0.0293]	6421 [R_{int} = 0.0583]	6066 [R_{int} = 0.0000]
Completeness to θ	65.50°, 95.7 %	25.02°, 98.6 %	66.59°, 96.3 %	66.50°, 94.8 %
Max. and min. transmission	0.2637 and 0.1247	0.8620 and 0.7329	0.7528 and 0.4551	0.6157 and 0.5789
Largest difference peak and hole [e Å^{-3}]	1.011 and –1.082	0.465 and –0.314	1.353 and –0.844	0.790 and –0.494
Data/restraints/parameters	5676/0/424	6286/0/423	6421/0/442	6066/0/320
Goodness-of-fit on F^2	1.057	1.058	1.033	1.048
Final R indices	$R1$ = 0.0393,	$R1$ = 0.0289,	R_1 = 0.0384,	$R1$ = 0.0450,
[$F^2 > 2\sigma(F^2)$]	$wR2$ = 0.1018	$wR2$ = 0.0696	wR_2 = 0.1047	$wR2$ = 0.1083
R indices	$R1$ = 0.0396,	$R1$ = 0.0374,	R_1 = 0.0389,	$R1$ = 0.0580,
(all data)	$wR2$ 0.1022	$wR2$ = 0.0733	wR_2 = 0.1055	$wR2$ 0.1132

	2·DMF/DMSO	**2**·EtOAc	**2**·THF
Empirical formula	$C_{28}H_{44}B_{10}Cl_4N_2O_4Pd_2$·2DMF·4DMSO	$C_{28}H_{44}B_{10}Cl_4N_2O_4Pd_2$· 7EtOAc	$C_{28}H_{44}B_{10}Cl_4N_2O_4Pd_2$·6THF
Formula weight	1530.18	1688.20	1504.10
Crystal system	triclinic	triclinic	monoclinic
Space group	$P\bar{1}$	$P\bar{1}$	$P2_1/c$
Unit cell dimensions [Å, °]	a = 11.0309(7)	a = 10.9184(4)	a = 15.8587(6)
	b = 11.8125(11)	b = 12.6486(4)	b = 20.1147(8)
	c = 15.1099(14)	c = 15.8324(5)	c = 10.9262(4)
	α = 112.497(5)	α = 78.2290(10)	
	β = 104.671(5)	β = 76.1020(10)	
	γ = 94.053(4)	γ = 80.3860(10)	
Volume [Å^3]	1728.5(3)	2061.77(12)	3466.1(25)
Z	1	1	2
$\varrho_{calcd.}$ [g cm^{-3}]	1.470	1.360	1.441
Absorption coeff. [mm^{-1}]	7.173	5.212	0.728
F(000)	780	868	1544
Crystal	block, yellow	block, yellow	block, yellow
Crystal size [mm]	0.1 × 0.08 × 0.04	0.12 × 0.08 × 0.08	0.14 × 0.11 × 0.1
θ range for data collection [°]	3.32–66.81	2.92–71.05	2.39–25.00
Reflections collected	16633	26681	33606
Independent reflections	5933 [R_{int} = 0.0489]	7702 [R_{int} = 0.0354]	6068 [R_{int} = 0.1022]
Completeness to θ	66.50°, 97.8 %	70.64°, 97.4 %	25.00°, 99.3 %
Max. and min. transmission	0.7624 and 0.5340	0.6806 and 0.5736	0.9307 and 0.9049
Largest difference peak and hole [e Å^{-3}]	1.811 and –1.037	0.468 and –0.427	1.256 and –1.287
Data/restraints/parameters	5933/0/367	7702/0/394	6068/4/410
Goodness-of-fit on F^2	1.061	1.043	1.046
Final R indices [$F^2 > 2\sigma(F^2)$]	$R1$ = 0.0442, $wR2$ = 0.1173	$R1$ = 0.0256, $wR2$ = 0.0682	R_1 = 0.0556, $wR2$ = 0.1179
R indices (all data)	$R1$ = 0.0468, $wR2$ = 0.1207	$R1$ = 0.0269, $wR2$ = 0.0704	R_1 = 0.0896, $wR2$ = 0.1327

Table 2. Details for solvents of crystallization, host/guest stoichiometry, space group, calculated density (D [mg m^{-3}]), guest-accessible volume (V [% unit cell]).[a]

Inclusion compound	Solvent of crystallization	Host/guest	Space group	D	V
2·DMF-I	DMF	1:6	$P\bar{1}$	1.454	36
2·DMF-II	DMF	1:6	$P2_1/n$	1.390	42
2·DMSO-I	DMSO	1:8	$P\bar{1}$	1.490	47
2·DMSO-II	DMSO	1:7[b]	$P2_1/n$	1.485	41
2·DMF/DMSO	DMF + DMSO	1:2+4[b]	$P\bar{1}$	1.470	36
2·EtOAc	EtOAc	1:7[b]	$P\bar{1}$	1.360	53
2·THF	THF	1:6	$P2_1/c$	1.441	39

[a] Calculated in mercury (probe radius 1.2 Å; grid spacing 0.7 Å) after removing the solvent from the structures. [b] Olex2 was used to remove the electronic contribution of disordered solvent molecules per host: 5 DMSO molecules in **2**·DMSO-II, 2 DMSO molecules in **2**·DMF/DMSO, and 3 EtOAc molecules in **2**·EtOAc.

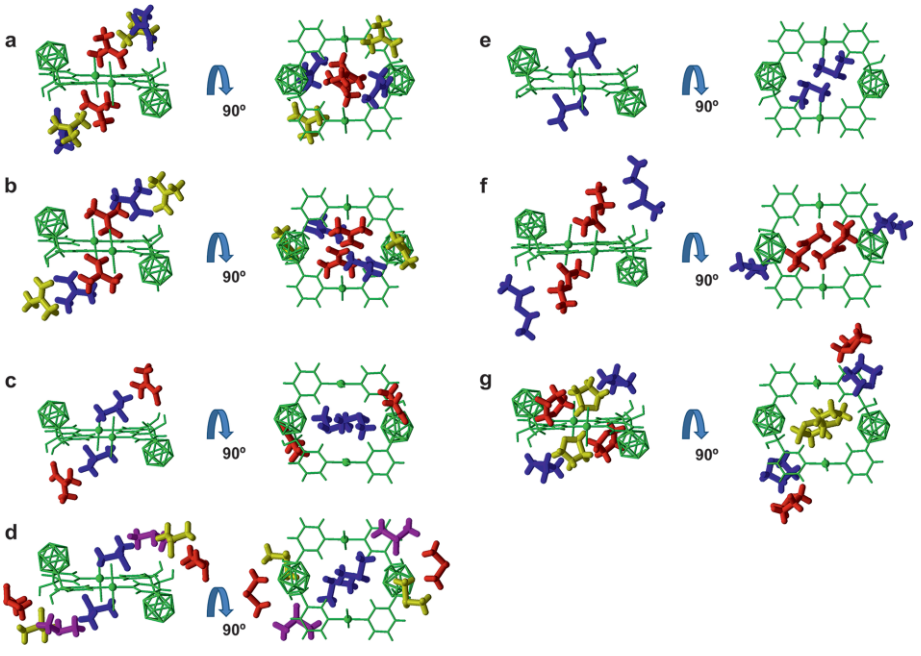

Figure 3. Plots of the SCXRD crystal structures for: (a) **2**·DMF-I; (b) **2**·DMF-II; (c) **2**·DMF/DMSO; (d) **2**·DMSO-I; (e) **2**·DMSO-II; (f) **2**·EtOAc; and (g) **2**·THF. Two orthogonal projections are shown for each palladacycle molecule, shown in green. Solvent molecules are shown with colors corresponding to the equivalent sites. Hydrogen atoms in the carborane cluster are omitted for clarity.

2.65–2.77 Å and 147–177°, respectively). The *in-* and *out-guest* molecules are, however, interacting with the host by weaker hydrogen bonds of the type (host)C–H···O/Cl(guest) and C–H···H–B intermolecular contacts. The intermolecular contacts C–H···O (H···O 2.20–2.69, C–H–O 134–166°), C–H···Cl (H···Cl 2.69–2.93, C–H–Cl 115–162°), and C–H···H–B (H···H 2.22–2.35, C–H–H 98–154°, H–H–B 128–157°) are found. Significant guest–guest hydrogen bonding is also observed in the structures through C–H···O interactions (Table 3). The inclusion compound **2**·DMF/DMSO deserves some comments, as contrary to all other structures, it contains two guest molecules of different nature. In this particular structure, DMF and DMSO are acting as *on-guest* and *in-guest* molecules, respectively. This means that the more-polar and better hydrogen-bond-acceptor DMSO guest is occupying the site dominated by weaker C–H···O hydrogen bonding, whereas a somewhat worse hydrogen-bond acceptor, such as DMF, is occupying the moderate O–H···O hydrogen-bonding sites.[18]

Owing to the large amount of solvent molecules per guest, the palladacycles of **2** are well-surrounded by the solvent molecules in a sort of "supramolecular soup". Figure 4 shows a representation of the 3D structure for all of these compounds, in which the solvent molecules are omitted for clarity. Therefore, in this representation, only host–host interactions are emphasized.

All inclusion compounds, except that for **2**·THF, show a similar arrangement of the palladacyclic rings in the 3D structure (Figure 4). That is, palladacycles of **2** tend to organize in 2D layers when crystallized in highly polar solvents (DMF, DMSO, DMF/DMSO, or EtOAc). In the latter, palladacycles of **2** seem to rotate in the 2D planes by optimizing the C–H···O and/or C–H···Cl interactions (Table 3 and Figures S4–S6), thus facilitating different relative orientation of rings and different crystal forms (e.g., **2**·DMSO-I vs. **2**·DMSO-II). These 2D supramolecular layers are "floating" on the solvent, but segregate in a columnar mode (**2**·DMF-I, **2**·DMSO-I, **2**·DMF/DMSO, **2**·EtOAc, and **2**·DMSO-

Table 3. Geometrical parameters of host–guest and guest–guest contacts involved in the **2**·solvent structures.

Compound	D–H···A[a]	*d*(D···A) [Å]	*d*(H···A) [Å]	∠(DHA) [°]	∠(HHB) [°]
2·DMF-I	**host–guest**				
		***on*-guest**			
	O(22)–H···O(41)	2.742(3)	1.90	176.6	–
	O(14)–H···O(31)	2.777(3)	2.04	146.8	–
		***in*-guest**			
	C(13)–H···O(31)	3.022(3)	2.59	106.0	–
	C(13)–H···O(51)	3.344(4)	2.41	154.6	–
	C(20)–H···O(51)	3.403(3)	2.55	149.2	–
	C(21)–H···O(51)	3.269(3)	2.37	149.8	–
	C(28)–H···O(51)	3.208(3)	2.38	146.2	–
	C(54)–H(B)···H–B(8)[i]	4.151(7)	2.35	154.0	134.4
		***out*-guest**			
	C(25)–H···O(31)[ii]	3.278(4)	2.48	141.9	–
	guest–guest				
	C(32)–H···O(41)	3.469(4)	2.59	153.5	–
	C(52)–H···O(31)	3.339(4)	2.58	137.4	–
	host–host				
	C(26)–H···Cl(1)[iii]	3.668(4)	2.85	145.0	–
	C(24)–H···O(22)[iii]	3.282(3)	2.49	141.5	–
2·DMF-II	**host–guest**				
		***on*-guest**			
	O(22)–H···O(31)	2.651(2)	1.82	172.0	–
	O(14)–H···O(41)	2.714(2)	1.90	163.6	–
	C(32)–H···O(14)	3.332(3)	2.71	124.0	–
		***in*-guest**			
	C(13)–H···O(51)[i]	3.344(3)	2.38	161.7	–
	C(20)–H···O(51)[i]	3.397(3)	2.54	150.0	–
	C(28)–H···O(51)[i]	3.249(3)	2.36	156.5	–
	C(44)–H(C)···Cl(2)	3.465(3)	2.93	115.0	–
	B(3)–H(B)···O(51)[i]	3.546(3)	2.70	131.7	–
		***out*-guest**			
	C(25)–H···O(41)[iv]	3.186(3)	2.38	142.5	–
	guest–guest				
	C(42)–H···O(51)[i]	3.399(3)	2.46	171.2	–
	host–host				
	C(26)–H···Cl(2)[iv]	3.734(3)	2.94	142.5	–
	C(17)–H···H–B(7)[v]	2.355	2.36	118.4	131.0
2·DMSO-I	**host–guest**				
		***on*-guest**			
	O(14)–H···O(32)[vi]	2.628(3)	1.81	164.8	–
	O(22)–H···O(42)	2.760(3)	1.93	169.9	–
		***in*-guest**			
	C(20)–H···O(2)	3.197(4)	2.29	159.6	–
	C(21)–H···O(2)	3.167(3)	2.20	163.5	–
	C(28)–H···O(2)	3.330(4)	2.60	133.9	–
	C(4)–H(C)···Cl(2)	3.764(4)	2.90	148.2	–
	C(3)–H(C)···Cl(1)[vii]	3.577(4)	2.88	129.2	–
	C(3)–H(C)···H–B(3)[ii]	3.442(4)	2.29	98.2	127.9
		***out*-guest**			
	C(00W)–H(B)···O(14)	3.473(4)	2.72	134.2	–
	C(00)–H(D)···O(22)	3.408(3)	2.47	159.6	–
	guest–guest				
	C(4)–H(A)···O(42)	3.421(4)	2.45	170.8	–
	host–host				
	C(18)–H···Cl(1)[iv]	3.715(3)	2.93	140.6	–
	C(26)–H···Cl(1)[vii]	3.557(4)	2.70	149.8	–
	C(16)–H···H–B(9)[i]	3.159	2.30	149.8	137.2

Table 3. (*Continued*.)

Compound	D–H···A[a]	*d*(D···A) [Å]	*d*(H···A) [Å]	∠(DHA) [°]	∠(HHB) [°]
2·DMSO-II	**host–guest**				
		***in*-guest**			
	C(13)–H···O(2)	3.224(5)	2.28	157.7	–
	C(20)–H···O(2)	3.327(5)	2.50	145.1	–
	C(21)–H···O(2)	3.330(7)	2.42	150.6	–
	C(28)–H···O(2)	3.198(5)	2.35	148.0	–
	C(3)–H(C)···H–B(3)i	3.858(7)	2.27	131.0	147.5
	host–host				
	C(26)–H···O(14)^{viii}	3.308(7)	2.52	140.8	–
2·DMF/DMSO	**host–guest**				
		***on*-guest**			
	O(14)–H···O(41)	2.787(5)	1.97	162.4	–
	O(22)–H···O(41)	2.688(5)	1.93	150.0	–
	C(21)–H···O(41)	3.129(6)	2.61	112.5	–
		***in*-guest**			
	C(13)–H···O(31)	3.268(6)	2.34	154.0	–
	C(20)–H···O(31)^{ix}	3.279(6)	2.42	149.7	–
	C(21)–H···O(31)	3.362(4)	2.47	148.2	–
	C(28)–H···O(31)	3.200(5)	2.35	148.2	–
	C(34A)–H···Cl(2)	3.837(6)	2.89	161.9	–
	C(33)–H(A)···H–B(6)^{ix}	3.611(5)	2.22	106.8	156.7
	host–host				
	C(26)–H···Cl(1)^{x}	3.702(4)	2.85	149.3	–
	C(24)–H···O(22)^{xi}	3.370(4)	2.48	155.4	–
2·EtOAc	**host–guest**				
		***on*-guest**			
	O(22)–H···O(41)^{xi}	2.747(2)	1.91	172.1	–
	C(43)–H(A)···O(22)^{xi}	3.206(3)	2.58	121.9	–
		***in*-guest**			
	C(13)–H···O(31)^{ii}	3.389(2)	2.49	149.8	–
	C(20)–H···O(31)^{ii}	3.295(2)	2.55	135.8	–
	C(21)–H···O(31)^{ii}	3.378(3)	2.42	161.4	–
	C(28)–H···O(31)^{ii}	3.511(3)	2.69	144.9	–
		***out*-guest**			
	C(17)–H···O(41)^{xii}	3.433(3)	2.50	169.4	–
	C(43C)–H···O(14)^{xiii}	3.421(3)	2.59	142.6	–
	host–host				
	C(18)–H···Cl(2)^{vi}	3.725(2)	2.92	143.9	–
	C(25)–H···H–B(5)^{ii}	2.952	2.41	115.7	122.8
2·THF	**host–guest**				
		***on*-guest**			
	O(22)–H···O(29)	2.737(5)	1.90	171.6	–
		***in*-guest**			
	C(20)–H···O(39)^{i}	3.307(7)	2.38	166.1	–
	C(21)–H···O(39)^{i}	3.553(6)	2.58	165.4	–
	C(41)–H(B)···Cl	3.629(8)	2.69	158.7	–
	C(43)–H(A)···H–B(3)	3.995(9)	2.33	132.0	151.1
		***out*-guest**			
	C(25)–H···O(34)^{xiv}	3.116(6)	2.53	120.5	–
	C(26)–H···O(34)^{xiv}	3.146(6)	2.57	119.7	–
	host–host				
	O(14)–H···Cl(2)^{vii}	3.115(4)	2.33	155.3	–

[a] O–H bond lengths are not normalized to neutron distances. Symmetry codes: (i) 1 – *x*, 1 – *y*, 1 – *z*; (ii) 1 + *x*, +*y*, +*z*; (iii) 2 – *x*, 1 – *y*, 1 – *z*; (iv) +*x*, 1 + *y*, +*z*; (v) +*x*, –1 + *y*, +*z*; (vi) –1 + *x*, +*y*, +*z*; (vii) 1 – *x*, 1 – *y*, 2 – *z*; (viii) –1/2 + *x*, 3/2 – *y*, –1/2 + *z*; (ix) 2 – *x*, 2 – *y*, 1 – *z*; (*x*) 1 – *x*, 2 – *y*, 1 – *z*; (xi) 1 – *x*, 1 – *y*, –*z*; (xii) 1 – *x*, –*y*, 1 – *z*; (xiii) +*x*, +*y*, –1 + *z*; (xiv) –1 + *x*, +*y*, –1 + *z*.

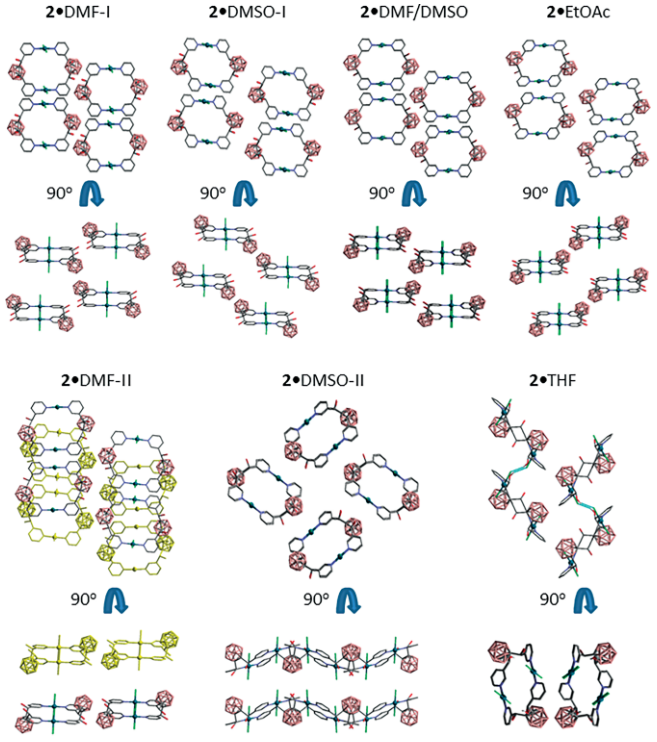

Figure 4. Molecular arrangements of **2** in the 3D structures. Projections showing eight molecules of **2** for each inclusion compound: **2**•DMF-I (top/bottom) along the *b*/*a* axis; **2**•DMSO-I (top/bottom) along the a/*b* axis; **2**•DMF/DMSO (top/bottom) along the *b*/*c* axis; **2**•EtOAc (top/bottom) along the *b*/*c* axis; **2**•DMF-II (top) between the *a* and *c* axes, (bottom) along the *b* axis; **2**•DMSO-II (top) along the *a* axis, (bottom) between the *a* and *c* axes; **2**•THF (top/bottom) along the *a*/*c* axis. All hydrogen atoms, except those hydrogen-bonded in **2**•THF, and all solvent molecules are omitted for clarity. Color code: B pink; C grey; H white; O red; N blue; Cl green; the blue dotted lines are hydrogen bonds.

II), leading to interstitial channels perpendicular to the palladacyclic rings, or segregate in a offset or slipped manner (**2**•DMF-II, Figure 4). This interlayer movement can also be the origin of polymorphism (e.g., **2**•DMF-I vs. **2**•DMF-II). The interlayer distances can also vary significantly (ca. 0–4 Å), according to the solvent included in the structures. As mentioned above, the 3D structure for **2**•THF is significantly different from all others in this work. In this case, supramolecular hydrogen-bonded O–H···Cl 1D chains are formed (Figure 3). An examination of the supramolecular network for this inclusion compound already reveals that dense packing for an apohost (unsolvated **2**) would be difficult. The awkward shape of host **2** does not facilitate self-assembly. Thus, hydrogen-bonded O–H···Cl 1D chains of **2** are assembled in combination with THF to provide the 3D structure. In spite of our efforts, we were not able to obtain an unsolvated form of **2** (the apohost).

Conclusion

We have reported the synthesis and characterization of a new palladacycle (**2**) obtained from the reaction between bis[3-pyridyl(hydroxy)methyl]-1,2-dicarba-*closo*-dodecaborane and $[PdCl_2(CH_3CN)_2]$. Compound **2** acts as a host for seven crystalline inclusion compounds from DMF, DMSO, EtOAc, and THF. The exceptional ratio of host/guest 1:*n* (*n* = 6–8) indicates a high efficiency of guest accommodation. Host **2** shows affinity for polar guest molecules, due to the presence of a large number of host–guest interactions (O–H···O, C–H···Cl, C–H···O, and weak C–H···H–B). The presence of the *o*-carboranyl moieties in host **2** seems to provide improved inclusion properties, with high stoichiometric ratios of the solvent included. This could be beneficial for designing hosts with storage or sensing properties.

Experimental Section

General: Reactions were carried out under air in capped vials. DMF, THF, DMSO, and EtOAc were commercially available and were used as received. The *syn*-diastereoisomer of 1,2-bis[(pyridin-3-yl)methanol]-1,2-dicarba-*closo*-dodecaborane (**1**) was synthesized according to the reported method.[9c] FTIR ATR spectra were recorded with a Perkin–Elmer Spectrum One spectrometer. The ^1H and ^{11}B spectra were recorded at 300 and 96 MHz, respectively, with a Bruker Advance-300 spectrometer in deuterated DMSO, unless denoted, and were referenced to the residual solvent peak for ^1H and $^{13}C\{^1H\}$ NMR or to BF_3OEt_2 as the external standard for ^{11}B NMR spectroscopy. Chemical shifts are reported in ppm and coupling constants are in Hertz. Multiplet nomenclature is as follows: s, singlet; d, doublet; t, triplet; br, broad; m, multiplet. Elemental analyses were obtained with a CarboErba EA1108 microanalyzer (Universidad Antonoma de Barcelona).

Synthesis of $[Pd_2Cl_2(1)_2]$·DMF (2·DMF): Compound **1** (200 mg, 0.558 mmol) and $[PdCl_2(MeCN)_2]$ (122mg, 0.558 mmol) were mixed in DMF (3 mL) in an open vial at ambient temperature and stirred until a clear yellow solution was obtained. The clear solution was allowed to stand and yellow crystals were obtained after two days (341.7 mg, 0.227 mmol, 81.5 %). Concomitant crystallization of polymorphs was observed by single-crystal X-ray diffraction, as habits for the crystals were very similar and could not be distinguished by visual inspection. ^1H NMR ([D$_6$]DMSO): δ = 9.34 (s, 1 H, NC_5H_4), 8.82 [d, $^3J_{H,H}$ = 6.0 Hz, 1 H, NC_5H_4], 8.16 [d, $^3J_{H,H}$ = 9.0 Hz, 1 H, NC_5H_4], 7.69 [dd, $^3J_{H,H}$ = 9.0 and 6.0 Hz, 1 H, NC_5H_4], 6.95 [d, $^3J_{H,H}$ = 6.0 Hz, 1 H, OH], 6.11 [d, $^3J_{H,H}$ = 6.0 Hz, 1 H, CH] ppm. ^{11}B NMR ([D$_6$]DMSO): δ = –8.87 (s, 10 B) ppm. IR (ATR; selected bands): $\tilde{\nu}$ = 3218 (OH), 2564 (BH), 1652 (C=O from DMF) cm^{-1}.

Synthesis of $[Pd_2Cl_2(1)_2]$·DMSO (2·DMSO): A similar procedure to that above, using **1** (50 mg, 0.139 mmol), $[PdCl_2(MeCN)_2]$ (30.5 mg, 0.139 mmol), and DMSO (1.5 mL), afforded yellow crystals after one day (64.9 mg, 0.048 mmol, 70 %). IR (ATR; selected bands): $\tilde{\nu}$ = 3242 (OH), 2609, 2567 (BH), 1024 (S=O from DMSO) cm^{-1}. Concomitant crystallization of polymorphs was observed by single-crystal X-ray diffraction, as habits for the crystals were very similar and could not be distinguish by visual inspection.

Recrystallization of 2·DMF: Crystals from **2·DMF** (40 mg, 0.027 mmol) were recrystallized from the appropriate solvent (12 mL). Crystals were obtained in after 1–2 days from THF (**2·THF**), EtOAc (**2·EtOAc**), and DMF/DMSO in a 1:1 ratio (**2·DMF/DMSO**). IR (ATR; selected bands, **2·THF**): $\tilde{\nu}$ = 3226 (OH), 2975, 2865 (THF), 2575 (BH). IR (ATR; selected bands, **2·EtOAc**): $\tilde{\nu}$ = 3220 (OH), 2579 (BH), 1713, 1250 (S=O from EtOAc) cm^{-1}. IR (ATR; selected bands, **2·DMF/DMSO**): $\tilde{\nu}$ = 3323, 3240 (OH), 2609, 2567 (BH), 1649 (C=O from DMF), 1024 (S=O from DMSO) cm^{-1}.

Single-Crystal X-ray Diffraction: Measured crystals were prepared under inert conditions and were immersed in perfluoropolyether as

a protective oil for manipulation. Suitable crystals were mounted on MiTeGen Micromounts™ and these samples were used for data collection. Data were collected with Bruker X8 Proteum (compounds **2**·DMF-I and **2**·DMSO-I) or Bruker D8 Venture (**2**·DMF-II, **2**·DMSO-II, **2**·DMF/DMSO, **2**·EtOAc, and **2**·THF) diffractometers. The data were processed with the APEX2 program[19] and were corrected for absorption using SADABS.[20] The structures were solved by direct methods,[21] which revealed the position of all non-hydrogen atoms. These atoms were refined on F^2 by a full-matrix least-squares procedure using anisotropic displacement parameters. All hydrogen atoms were located in difference Fourier maps and were included as fixed contributions riding on attached atoms with isotropic thermal displacement parameters 1.2 (C–H, B–H) or 1.5 (O–H) times those of the respective atom. A summary of the crystal data is reported in Table 1. In **2**·DMSO-I, one DMSO molecule was disordered over two positions in a 0.80:0.20 ratio. In **2**·THF, two THF molecules were disordered over two positions and their occupancies were refined (0.58:0.42 and 0.54:0.46, respectively). Some DMSO (**2**·DMSO-II and **2**·DMF/DMSO) and ethyl acetate (**2**·EtOAc) solvent molecules were highly disordered, so that the solvent-masking procedure implemented in Olex2[16] was used to remove the electronic contribution of these molecules from the refinement. CCDC 1546629 (for **2**·DMF-I), 1546630 (for **2**·DMF-II), 1546631 (for **2**·DMSO-I), 1546632 (for **2**·DMSO-II), 1546633 (for **2**·DMF/DMSO), 1546634 (for **2**·EtOAc), and 1546635 (for **2**·THF) contain the supplementary crystallographic data for this paper. These data can be obtained free of charge from The Cambridge Crystallographic Data Centre.

Acknowledgments

We thank the Ministerio de Educación y Ciencia (MEC) grant CTQ2013-44670-R and the Generalitat de Catalunya (2014/SGR/149) for financial support. The project "Factoría de Cristalización, CONSOLIDER INGENIO-2010" provided X-ray structure facilities for this work. ICMAB acknowledges the support of the Ministerio de Economía y Competitividad (MINECO), Spain through the Severo Ochoa Centers of Excellence Program, under grant SEV-2015-0496.

Keywords: Carboranes · Lattice-inclusion compounds · Palladacycles · Host–guest systems · Metallacycles

[1] a) J. J. Vittal, M. Zaworotko, E. R. T. Tiekink, *Organic Crystal Engineering*, Wiley, New York, **2010**; b) J. W. Steed, J. L. Atwood, *Supramolecular Chemistry*, 2nd ed., Wiley, Chichester, **2009**; c) D. Braga, F. Creponi, *Making Crystals by Design: Methods, Techniques and Applications*, Wiley-VCH, Weinheim, Germany, **2007**; d) G. R. Desiraju, T. Steiner, *The Weak Hydrogen Bond in Structural Chemistry and Biology*, Oxford University Press, Oxford, **2001**; e) G. R. Desiraju, *Crystal Engineering: The Design of Organic Solids*, Elsevier Science Publishers B. V., Amsterdam, **1989**; f) M. C. Etter, *Acc. Chem. Res.* **1990**, *23*, 120–126.

[2] a) A. Ruffani, W. Seichter, A. Schwarzer, E. Weber, *Cryst. Growth Des.* **2016**, *16*, 3826–3837; b) R. Bishop, "Synthetic Clathrate Systems" in *Supramolecular Chemistry: from Molecules to Nanomaterials Vol. 6*, Wiley, Chichester, **2012**; c) L. R. Nassimbeni, *Encyclopedia of Supramolecular Chemistry*, CRC Press, Boca Raton, **2004**; d) *Comprehensive Supramolecular Chemistry* (Ed.: J. L. Atwood), Elsevier, Oxford, **1996**; e) E. Weber, *Comprehensive Supramolecular Chemistry Vol. 6*, Elsevier, Oxford, **1996**; f) E. C. Weber, "Molecular Inclusion and Molecular Recognition – Clathrates II", *Topics in Current Chemistry Vol. 149*, Springer-Verlag, Berlin, **1988**.

[3] D. V. Soldatov, *J. Chem. Crystallogr.* **2006**, *36*, 747–768.

[4] a) F. Toda, D. L. Ward, H. Hart, *Tetrahedron Lett.* **1981**, *22*, 3865–3868; b) F. Toda, K. Akagi, *Tetrahedron Lett.* **1968**, *9*, 3695–3698.

[5] F. Katzsch, T. Gruber, E. Weber, *Cryst. Growth Des.* **2015**, *15*, 5047–5061.

[6] a) F. Katzsch, E. Weber, *CrystEngComm* **2015**, *17*, 2737–2753; b) F. Maharaj, R. Bishop, D. C. Craig, P. Jensen, M. L. Scudder, N. Kumar, *Cryst. Growth Des.* **2009**, *9*, 1334–1338; c) S. B. Sembiring, S. B. Colbran, R. Bishop, D. C. Craig, A. D. Rae, *Inorg. Chim. Acta* **1995**, *228*, 109–117.

[7] a) A. Bacchi, P. Pelagatti, *Chem. Commun.* **2016**, *52*, 1327–1337; b) A. Bacchi, M. Carcelli, in *Science of Crystal Structures: Highlights in Crystallography*, **2015**, pp. 299–308.

[8] a) N. L. S. Yue, M. C. Jennings, R. J. Puddephatt, *Polyhedron* **2016**, *108*, 67–73; b) A. De León, M. Guerrero, J. García-Antón, J. Ros, M. Font-Bardía, J. Pons, *CrystEngComm* **2013**, *15*, 1762–1771; c) R. W. Troff, R. Hovorka, T. Weilandt, A. Lutzen, M. Cetina, M. Nieger, D. Lentz, K. Rissanen, C. A. Schalley, *Dalton Trans.* **2012**, *41*, 8410–8420; d) Q. Zhang, L. He, J.-M. Liu, W. Wang, J. Zhang, C.-Y. Su, *Dalton Trans.* **2010**, *39*, 11171–11179; e) M. Guerrero, J. Pons, V. Branchadell, T. Parella, X. Solans, M. Font-Bardia, J. Ros, *Inorg. Chem.* **2008**, *47*, 11084–11094; f) N. L. S. Yue, D. J. Eisler, M. C. Jennings, R. J. Puddephatt, *Inorg. Chem.* **2004**, *43*, 7671–7681

[9] a) S. Rodriguez-Hermida, M. Y. Tsang, C. Vignatti, K. C. Stylianou, V. Guillerm, J. Perez-Carvajal, F. Teixidor, C. Vinas, D. Choquesillo-Lazarte, C. Verdugo-Escamilla, I. Peral, J. Juanhuix, A. Verdaguer, I. Imaz, D. Maspoch, J. Giner Planas, *Angew. Chem. Int. Ed.* **2016**, *55*, 16049–16053; *Angew. Chem.* **2016**, *128*, 16283–16287; b) J. Planas, F. Teixidor, C. Viñas, *Crystals* **2016**, *6*, 50; c) F. Di Salvo, C. Paterakis, M. Y. Tsang, Y. Garcia, C. Viñas, F. Teixidor, J. Giner Planas, M. E. Light, M. B. Hursthouse, D. Choquesillo-Lazarte, *Cryst. Growth Des.* **2013**, *13*, 1473–1484.

[10] a) M. Y. Tsang, S. Rodríguez-Hermida, K. C. Stylianou, F. Tan, D. Negi, F. Teixidor, C. Viñas, D. Choquesillo-Lazarte, C. Verdugo-Escamilla, M. Guerrero, J. Sort, J. Juanhuix, D. Maspoch, J. Giner Planas, *Cryst. Growth Des.* **2017**, *17*, 846–857; b) See ref.[9b]; c) R. Núñez, I. Romero, F. Teixidor, C. Viñas, *Chem. Soc. Rev.* **2016**, *45*, 5147–5173; d) R. Núñez, M. Tarrés, A. Ferrer-Ugalde, F. F. De Biani, F. Teixidor, *Chem. Rev.* **2016**, *116*, 14307–14378; e) M. Y. Tsang, F. Teixidor, C. Viñas, D. Choquesillo-Lazarte, N. Aliaga-Alcalde, J. G. Planas, *Inorg. Chim. Acta* **2016**, *448*, 97–103; f) R. N. Grimes, in *Carboranes*, 3rd ed., Academic Press, Oxford, **2016**; g) M. Y. Tsang, C. Viñas, F. Teixidor, J. G. Planas, N. Conde, R. SanMartin, M. T. Herrero, E. Dominguez, A. Lledos, P. Vidossich, D. Choquesillo-Lazarte, *Inorg. Chem.* **2014**, *53*, 9284–9295; h) F. Di Salvo, M. Y. Tsang, F. Teixidor, C. Viñas, J. G. Planas, J. Crassous, N. Vanthuyne, N. Aliaga-Alcalde, E. Ruiz, G. Coquerel, S. Clevers, V. Dupray, D. Choquesillo-Lazarte, M. E. Light, M. B. Hursthouse, *Chem. Eur. J.* **2014**, *20*, 1081–1090; i) F. Di Salvo, F. Teixidor, C. Viñas, J. Giner Planas, *Z. Anorg. Allg. Chem.* **2013**, *639*, 1194–1198; j) R. Núñez, P. Farràs, F. Teixidor, C. Viñas, R. Sillanpää, R. Kivekäs, *Angew. Chem. Int. Ed.* **2006**, *45*, 1270–1272; *Angew. Chem.* **2006**, *118*, 1292.

[11] a) V. Terrasson, Y. García, P. Farràs, F. Teixidor, C. Viñas, J. G. Planas, D. Prim, M. E. Light, M. B. Hursthouse, *CrystEngComm* **2010**, *12*, 4109–4123; b) A. V. Puga, F. Teixidor, R. Sillanpää, R. Kivekäs, M. Arca, G. Barberà, C. Viñas, *Chem. Eur. J.* **2009**, *15*, 9755–9763; c) J. G. Planas, F. Teixidor, C. Viñas, M. E. Light, M. B. Hursthouse, *Chem. Eur. J.* **2007**, *13*, 2493–2502; d) J. Fanfrlík, M. Lepšík, D. Horinek, Z. Havlas, P. Hobza, *ChemPhysChem* **2006**, *7*, 1100–1105; e) J. G. Planas, C. Viñas, F. Teixidor, A. Comas-Vives, G. Ujaque, A. Lledós, M. E. Light, M. B. Hursthouse, *J. Am. Chem. Soc.* **2005**, *127*, 15976–15982; f) M. A. Fox, A. K. Hughes, *Coord. Chem. Rev.* **2004**, *248*, 457–476; g) P. C. Andrews, C. L. Raston, *J. Organomet. Chem.* **2000**, *600*, 174–185; h) M. J. Hardie, C. L. Raston, *Chem. Commun.* **1999**, 1153–1163; i) P. C. Andrews, M. J. Hardie, C. L. Raston, *Coord. Chem. Rev.* **1999**, *189*, 169–198.

[12] a) J. M. Ludlow III, M. Tominaga, Y. Chujo, A. Schultz, X. Lu, T. Xie, K. Guo, C. N. Moorefield, C. Wesdemiotis, G. R. Newkome, *Dalton Trans.* **2014**, *43*, 9604–9611; b) B. H. Northrop, H.-B. Yang, P. J. Stang, *Chem. Commun.* **2008**, 5896–5908; c) H. Jude, H. Disteldorf, S. Fischer, T. Wedge, A. M. Hawkridge, A. M. Arif, M. F. Hawthorne, D. C. Muddiman, P. J. Stang, *J. Am. Chem. Soc.* **2005**, *127*, 12131–12139; d) N. Das, P. J. Stang, A. M. Arif, C. F. Campana, *J. Org. Chem.* **2005**, *70*, 10440–10446.

[13] a) M. Y. Tsang, F. Di Salvo, F. Teixidor, C. Viñas, J. Giner Planas, D. Choquesillo-Lazarte, N. Vanthuyne, *Cryst. Growth Des.* **2015**, *15*, 935–945; b) F. Di Salvo, F. Teixidor, C. Viñas, J. Giner Planas, M. E. Light, M. B. Hursthouse, N. Aliaga-Alcalde, *Cryst. Growth Des.* **2012**, *12*, 5720–5736; c) F. Di Salvo, B. Camargo, Y. Garcia, F. Teixidor, C. Viñas, J. Giner Planas, M. E. Light, M. B. Hursthouse, *CrystEngComm* **2011**, *13*, 5788–5806; d) J. G. Planas, C.

Vinas, F. Teixidor, M. E. Light, M. B. Hursthouse, *CrystEngComm* **2007**, *9*, 888–894.
[14] M. J. Bayer, A. Herzog, M. Diaz, G. A. Harakas, H. Lee, C. B. Knobler, M. F. Hawthorne, *Chem. Eur. J.* **2003**, *9*, 2732–2744.
[15] R. A. S. Vasdev, D. Preston, J. D. Crowley, *Dalton Trans.* **2017**, *46*, 2402–2414.
[16] O. V. Dolomanov, L. J. Bourhis, R. J. Gildea, J. A. K. Howard, H. Puschmann, *J. Appl. Crystallogr.* **2009**, *42*, 339–341.
[17] E. Weber, S. Nitsche, A. Wierig, I. Csöregh, *Eur. J. Org. Chem.* **2002**, 856–872.
[18] a) M. C. Foti, G. A. DiLabio, K. U. Ingold, *J. Am. Chem. Soc.* **2003**, *125*, 14642–14647; b) C. Laurence, M. Berthelot, *Perspect. Drug Discovery Des.* **2000**, *18*, 39–60; c) M. H. Abraham, P. L. Grellier, D. V. Prior, J. J. Morris, P. J. Taylor, *J. Chem. Soc. Perkin Trans. 2* **1990**, 521–529.
[19] A. S. Bruker, V 2012.2, Bruker AXS Inc., Madison, WI, **2012**.
[20] G. M. Sheldrick, *University of Göttingen, Germany*, **2012**.
[21] G. M. Sheldrick, *Acta Crystallogr., Sect. A: Found. Crystallogr.* **2008**, *64*, 112–122.

Received: May 11, 2017